Sensitivity Analysis of Transport Parameters Estimated from the Adsorption/Desorption Column Experiments to the Errors in Equilibrium Data*

I. TATÁROVÁ and M. POLAKOVIČ**

Department of Chemical and Biochemical Engineering, Faculty of Chemical and Food Technology, Slovak University of Technology, SK-812 37 Bratislava
e-mail: milan.polakovic@stuba.sk

Received 1 April 2004

Dedicated to the 80th birthday of Professor Elemír Kossaczký

This study focused on the problem of the systematic errors of the adsorbed/desorbed amount in column experiments when the parameters of the Langmuir isotherm were obtained from independent experiments. The effect of this discrepancy on the estimation of the mass transfer coefficient in the linear driving force model was investigated. The systematic errors were introduced by using the negatively or positively biased values of the partition coefficient from 1 % to 10 %. Simulated experiments were carried out with the biased values using a dimensionless form of the adsorption column model having three parameters: the dimensionless mass transfer coefficient (d), the partition coefficient (Λ), and the separation factor (r) that characterizes the degree of saturation of adsorbent. It was found interesting to vary a single model parameter, the product of d and Λ. Three values of $d\Lambda$, 50, 500, and 5000, were used. They covered the situations from an almost immediate breakthrough of the solute in the outlet to a sharp bend at negligible mass transfer resistance. The deviations of the estimated and true values of d were presented as functions of the systematic errors both for adsorption and desorption. The accuracies of the estimates of d were characterized by the t-values calculated from the residual sum of squares function.

The capacity and rate factors are key quantities in the fixed-bed adsorption. In different application areas, they constitute the basis for the selection of suitable adsorbents, design, and process optimization of plant adsorption units and for the analysis of their economical, long-term operation. High capacities of activated carbon for adsorption of organic molecules and low pollutant concentrations, however, result in a long duration of column experiments. For that reason, the experiments aimed at obtaining equilibrium and mass transport properties of adsorption systems have mostly been conducted in separate batch studies. Fixed-bed experiments were then conducted for the verification of models [1—3]. This is partly surprising since the exploitation of fixed-bed column techniques for the determination of adsorption equilibria is well established in the field of liquid-phase adsorption chromatography [4—6]. Several studies reported fitting of breakthrough curves for obtaining a transport parameter [7—9].

A problem can occur in the determination of transport parameters from adsorption/desorption profiles if the adsorption isotherm is obtained from independent measurements. The adsorbed or desorbed amount determined in a column experiment will never exactly match the value following from the adsorption isotherm for the given inlet solute concentration. The experimental and predicted profiles will then show a systematic deviation. The objective of this work was therefore to study the effect of these systematic errors on the accuracy and reliability of the estimation of the total mass transfer coefficient.

THEORETICAL

The mathematical model of the adsorption column consisted of the material balances of the liquid and solid phases and equilibrium relationship. They were all rearranged into dimensionless forms for the calculations performed in this study. The material balance

*Presented at the 31st International Conference of the Slovak Society of Chemical Engineering, Tatranské Matliare, 24—28 May 2004.
**The author to whom the correspondence should be addressed.

of the liquid phase had the following form

$$\frac{\partial c^*}{\partial \tau} + \Lambda \frac{\partial \bar{q}^*}{\partial \tau} + \frac{\partial c^*}{\partial \xi} = \frac{1}{Pe} \frac{\partial^2 c^*}{\partial \xi^2} \qquad (1)$$

where c^* and $\bar{q}^*$ are the dimensionless fluid phase and mean solid phase concentrations, respectively. The corresponding absolute concentration values were related to c_{ref} (the inlet fluid phase concentration at adsorption or the initial concentration at desorption) and q_{ref} (the equilibrium solid phase concentration to c_{ref}), respectively. ε is the void fraction of packing, $\Lambda = \rho_{\mathrm{b}} q_{\mathrm{ref}} / \varepsilon c_{\mathrm{ref}}$ the partition coefficient (ρ_{b} is the bulk density of packing), $Pe = \varepsilon v L / D_{\mathrm{L}}$ the Péclet number (v *is* the interstitial velocity, L the bed length, D_{L} the axial dispersion coefficient), $\tau = vt/L$ the dimensionless time (t is the time and L the bed length), and ζ the dimensionless bed axial coordinate related to L.

Two dominant terms in eqn (*1*) were the second and third ones on its left-hand side, the rate of adsorption of the species in the solid phase and the convection transport rate. The other two terms were not omitted for the reasons of the stability of numerical procedures. As a constant value of the partition coefficient $\Lambda = 1{,}000$ was used, the accumulation in fluid phase could essentially be neglected. Similarly, the Péclet number had the value of 1×10^7 which meant that the axial dispersion model, in effect, degenerated to the plug flow.

The material balance in the solid phase was based on the linear driving force model containing the total mass transfer coefficient (k_{S})

$$\frac{\partial \bar{q}^*}{\partial \tau} = d\,(q^* - \bar{q}^*) \qquad (2)$$

q^* is the dimensionless equilibrium solid phase concentration and $d = k_{\mathrm{S}} L a_{\mathrm{p}} / \varepsilon v$ the dimensionless mass transfer coefficient (a_{p} is the surface area per unit particle volume).

The adsorption isotherm was described by the Langmuir equation that, in the dimensionless form, contained a single parameter, separation factor $r = 1/(1 + c_{\mathrm{ref}} K)$ (K is the parameter of Langmuir isotherm)

$$q^* = \frac{c^*}{r + (1 - r)\, c^*} \qquad (3)$$

The initial and boundary conditions for the adsorption phase were

$$\tau = 0 \qquad c^* = \bar{q}^* = 0 \qquad (4)$$

$$\zeta = 0 \qquad c^* - \frac{1}{Pe} \frac{\partial c^*}{\partial \zeta} = 1 \qquad (5)$$

$$\zeta = 1 \qquad \frac{\partial c^*}{\partial \zeta} = 0 \qquad (6)$$

The initial and boundary conditions for the desorption phase were

$$\tau = 0 \qquad c^* = \bar{q}^* = 1 \qquad (7)$$

$$\zeta = 0 \qquad c^* - \frac{1}{Pe} \frac{\partial c^*}{\partial \zeta} = 0 \qquad (8)$$

$$\zeta = 1 \qquad \frac{\partial c^*}{\partial \zeta} = 0 \qquad (9)$$

EXPERIMENTAL

For a given set of parameters, the model was first applied to produce a set of simulated adsorption/desorption concentration profiles using a biased value of the partition coefficient Λ and the true value of the dimensionless mass transfer coefficient. The systematic errors of Λ were in the range from ± 1 % to ± 10 %. A correct value of Λ was then employed in the subsequent parameter estimation step where the simulated adsorption or desorption profile was fitted to get an estimated value of the dimensionless mass transfer coefficient. The investigation of the shape of the sum of squares function ($\xi^2 = f(d)$) was made to analyze the reliability of the estimation of d. The characteristic t-values were obtained as follows

$$t = \sqrt{\frac{\xi^2}{\hat{\xi}^2} - 1} \qquad (10)$$

where $\hat{\xi}^2$ is the minimum of the sum of squares function.

A commercial process engineering software, Athena Visual Workbench [10] (Stewart & Associates Engineering Software, Madison, WI; www.athenavisual.com), was used for all simulation and parameter estimation tasks in this study. The models were in the form of mixed (partial and ordinary) differential and algebraic equations with time discontinuities and were written in the user-friendly source code of the software. The details of numerical procedures incorporated in the Athena Visual Workbench can be found in original research papers [11, 12].

RESULTS AND DISCUSSION

The mathematical model introduced in the previous section contained three parameters – the dimensionless mass transfer coefficient d, the partition coefficient Λ, and the separation factor r. The use of the normalization of the liquid- and solid-phase concentrations introduced above caused that the adsorption/desorption profiles expressed in the dimensionless form were independent of the separation factor. For that reason, the single value of $r = 0.5$ was used in the study. A further reduction of the number of significant parameters was achieved by using the product

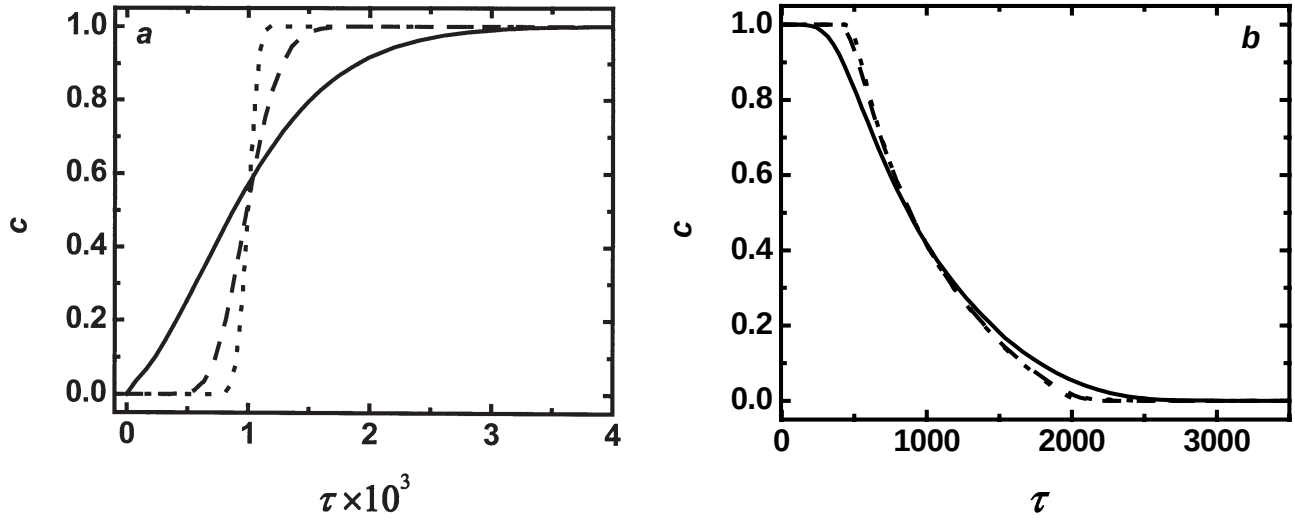

Fig. 1. The effect of the dimensionless mass transfer coefficient on the shape of *a*) adsorption and *b*) desorption profiles. Solid line – $d = 0.05$, dashed line – $d = 0.5$, dotted line – $d = 5$.

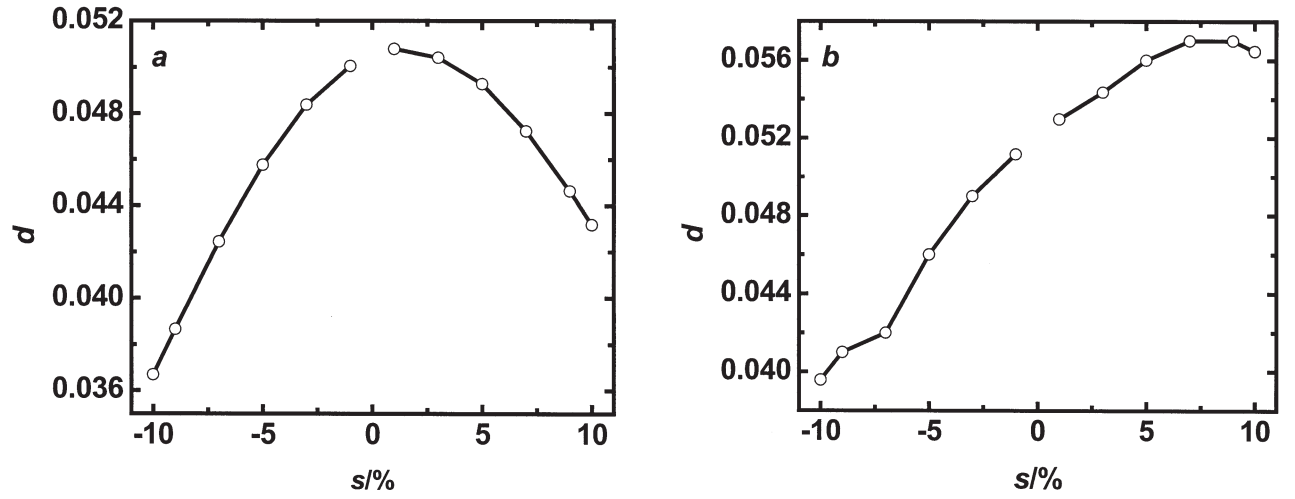

Fig. 2. Estimated value of d *vs.* the systematic error of Λ for *a*) adsorption and *b*) desorption. The true value d is equal to 0.05.

$d\Lambda$ as a parameter. The dimensionless concentration is then constant if it is plotted against the ratio of τ/Λ. We therefore decided to use a single value of Λ = 1,000 and to vary d.

The investigation of the effect of the mass transfer resistance was performed at the values of $d = 0.05$, 0.5, and 5. This range of the dimensionless mass transfer coefficients represents very distinct effects of the mass transfer resistance on the performance of adsorption column (Fig. 1*a*). At $d = 0.05$, the strong mass transfer resistance causes a widening of the adsorption zone throughout the whole column and immediate breakthrough. On the contrary, a negligible mass transfer resistance effect at $d = 5$ results in a very sharp adsorption zone and the self-sharpened shape of the breakthrough curve which is typical for the Langmuir isotherm. As it is well known at the Langmuir isotherm, the effect of mass transfer resistance is much smaller at the desorption profiles (Fig. 1*b*).

Fig. 2*a* presents the results of the sensitivity analysis for the adsorption profiles at $d = 0.05$. The estimated values of the dimensionless mass transfer coefficient are plotted as a function of the systematic error of the partition coefficient, s. It is interesting that d was underestimated in all but two cases. It means that the systematic error in Λ caused a widening of the predicted adsorption zone in order to accommodate the discrepancy between the true and predicted mean breakthrough times. Fig. 2*a* further shows that the deviations between the true and estimated values of d were not large. They did not exceed 25 % when they were larger at the negative systematic errors of Λ. In the case of desorption at the same d, the accuracy of estimation was slightly better than at adsorption and the deviations between true and estimated values of d had the same sign (except of $s = -1$ %) as the systematic errors of Λ (Fig. 2*b*).

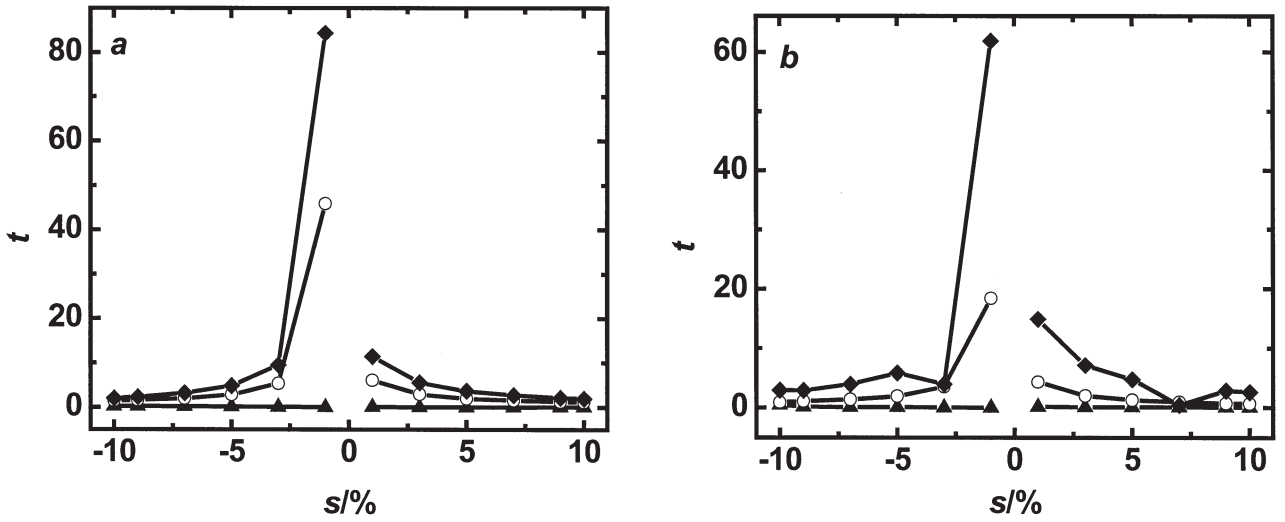

Fig. 3. Reliability of the estimation of d presented in Fig. 2 for a) adsorption and b) desorption. The individual lines are for the true value of d (triangles), $10d$ (circles), and $0.1d$ (squares).

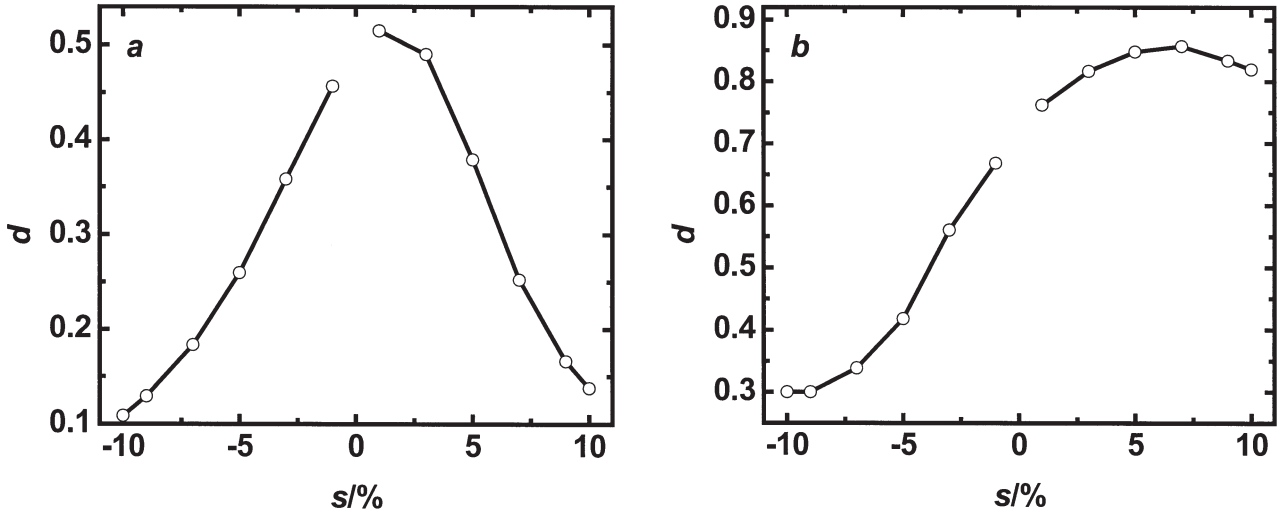

Fig. 4. Estimated value of d *vs.* the systematic error of Λ for a) adsorption and b) desorption. The true value of d is equal to 0.5.

Figs. 3a and 3b demonstrate the reliability of the estimation of d presented in Figs. 2a and 2b, respectively. In general, high t-values around the estimated d mean a very strong change of the sum of squares, ξ^2, with d and simultaneously a good accuracy of the estimate. Such results were obtained only if the absolute value of the systematic error was smaller than 3 %. At larger errors, the parametric sensitivity of ξ^2 with respect to d was significantly lower. This means that random errors could bias the estimates of d by tens of percent.

The accuracy of estimation of d was significantly worse when it was equal to 0.5. Fig. 4a shows that at adsorption phase, d was again mostly underestimated and it went down to about 20 % of the true value. It means that a significantly larger effect of mass transfer resistance had to be introduced to widen the breakthrough curve so that the discrepancy between the true and biased breakthrough points was accommodated. Fig. 4b shows that the accuracy of estimation was much better at desorption profiles. The deviations between the true and estimated values were distributed more symmetrically between the positive and negative values.

It follows from Figs. 5a and 5b that the reliabilities of estimation at $d = 0.5$ were much lower than at $d = 0.05$. A good sensitivity of ξ^2 in respect to d was observed only at the systematic errors of Λ equal to 1 % and 3 %. At adsorption, the good sensitivity was observed in both the positive and negative directions of the change of d (Fig. 5a) whereas, at desorption, the ξ^2-function was very little sensitive to the increase of d from the true value.

At the last value of the dimensionless mass transfer coefficient, $d = 5$, the procedure used could provide specific global optimal estimates of d only at adsorp-

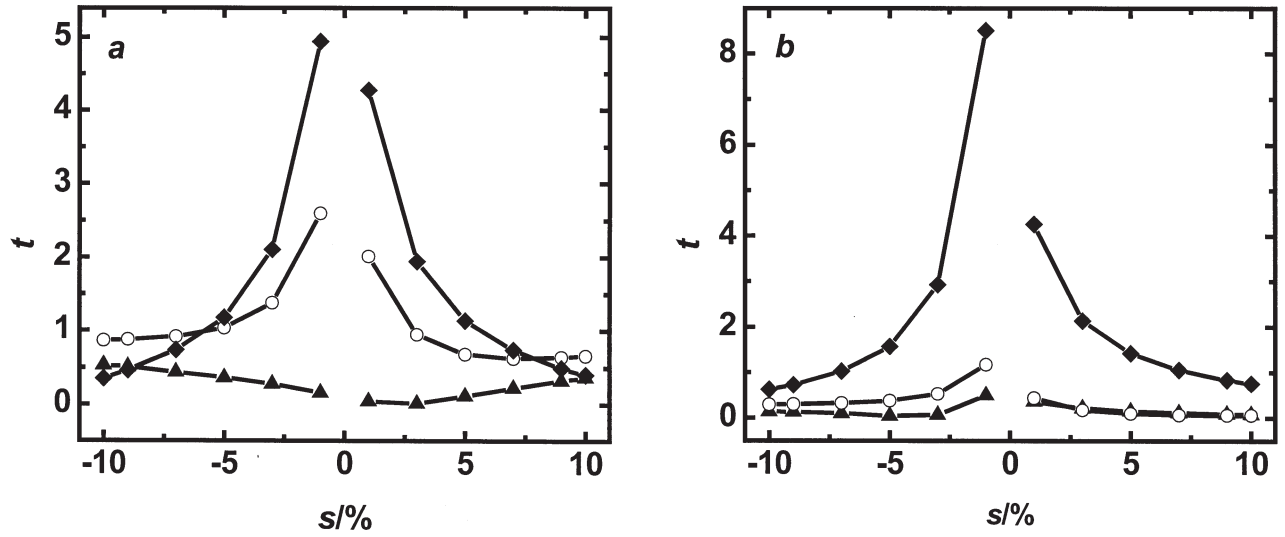

Fig. 5. Reliability of the estimation of d presented in Fig. 4 for *a*) adsorption and *b*) desorption. The individual lines are for the true value of d (triangles), $10d$ (circles), and $0.1d$ (squares).

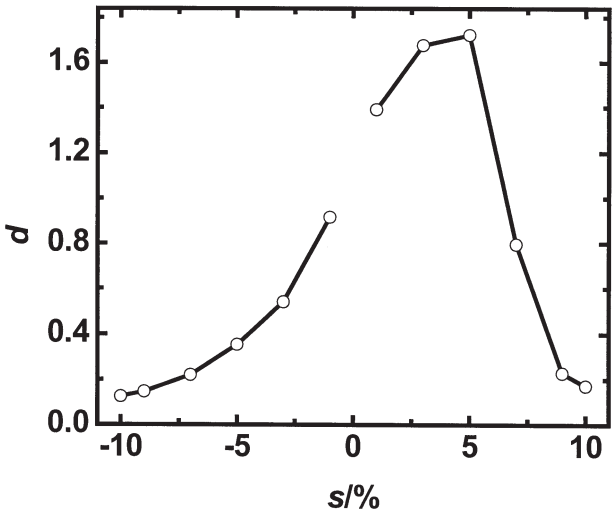

Fig. 6. Estimated value of d *vs.* the systematic error of Λ for adsorption at the true value of d equal to 5.

tion profiles (Fig. 6). At desorption, the ξ^2-function was essentially constant above certain values of d, so it was not possible to find a single minimum. The experimental and predicted desorption profiles therefore had the same shape and they were only shifted by a time period corresponding to the systematic error of Λ (Fig. 7*a*). Fig. 6 further shows that the accuracies of estimation at this dimensionless mass transfer coefficient were by far lower than at previous two values of d. At any value of systematic error of Λ, the estimates of d were smaller than 35 % of the true value. In many cases, they were lower more than ten times. An explanation of this result for the systematic error $s = +\ 10$ % follows from Fig. 7*b*. The experimental breakthrough curve (dotted line) was rather sharp whereas the estimated curve (solid line) was broadened, which enabled that the predicted and experimental curves came closer at the later phase of the breakthrough.

Fig. 8 shows that the t-values for $d = 5$ were by far lower than those presented in Figs. 3 and 5. As it has been mentioned above, at desorption, the sum of squares reached a plateau which is illustrated by the closeness of lines 1 and 2 in Fig. 8*b*. A very minor effect of the increase of d was observed at the adsorption profiles (lines 1 and 2 in Fig. 8*a*). This is understandable since already the true value of $d = 5$ represents a very low mass transfer resistance and so its increase cannot change much the shapes of adsorption profiles. However, the fluctuation of d towards lower values compared to the true one improved the quality of fit in most cases (line 3 is below line 1). This has already been explained in the discussion to Fig. 6. For that reason, there was no problem with finding an optimum estimate unlike at desorption.

An obvious conclusion of this study is that it may be troublesome to obtain good estimates of mass transfer parameters from the fixed-bed adsorption or desorption experiments. At the Langmuir isotherm, the use of adsorption profiles is much more convenient, since the desorption profiles are little sensitive to the change of mass transfer parameters. An adsorption profile with an early breakthrough seems to be almost a prerequisite for a reliable estimate of mass transfer coefficient. This condition has been employed in the so-called short-bed or zero-length column techniques. Of course, the application of these two techniques requires that other irregularities such as radial dispersion or proper development of axial flow or axial dispersion are treated.

Acknowledgements. This study was supported by the Slovak Grant Agency for Science VEGA (Grant No. 1/0065/03).

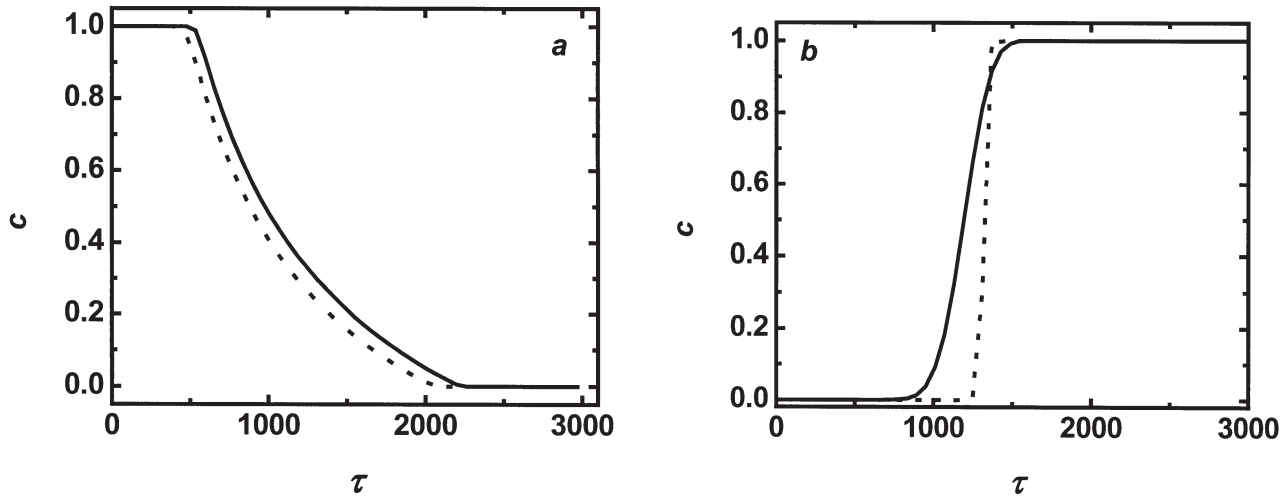

Fig. 7. Comparison of experimental (dotted line) and predicted (solid line) *a*) desorption and *b*) adsorption profiles at $d = 5$ and $s = +\ 10$ %.

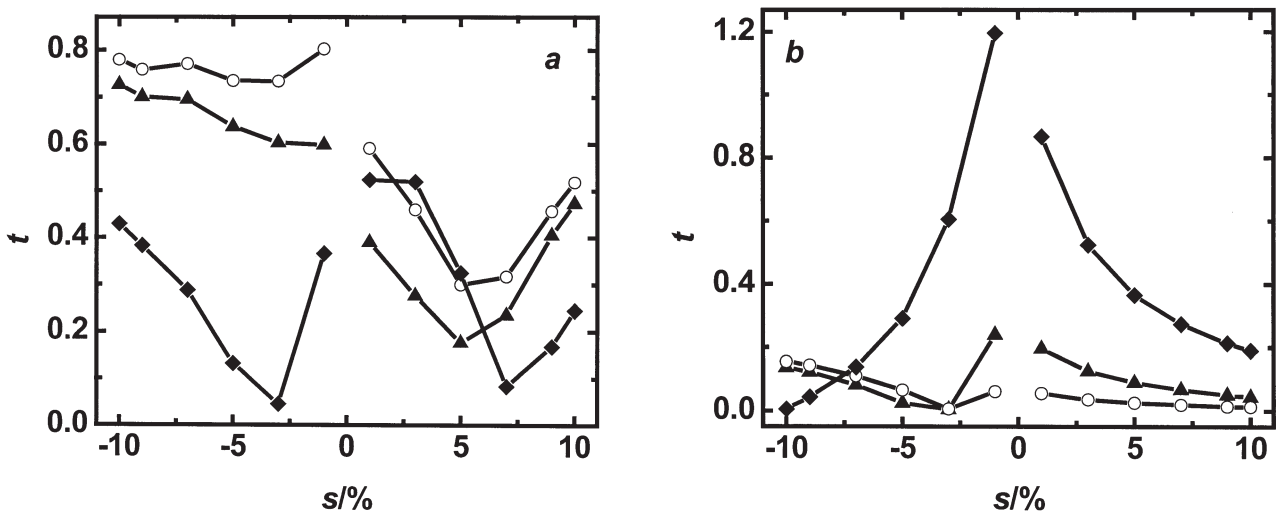

Fig. 8. Reliability of the estimation of d at the true value equal to 5. Fig. 8*a* corresponds to the estimation results presented in Fig. 6 for adsorption. Fig. 8*b* represents the change of the ξ^2-function with d at desorption. The individual lines are for the true value of d (triangles), $10d$ (circles), and $0.1d$ (squares).

SYMBOLS

a_p	specific surface area per unit particle volume	m^{-1}
Bi	dimensionless mass transfer coefficient ($= k_\mathrm{S} L a_\mathrm{p}/\varepsilon v$)	
c_ref	reference fluid-phase concentration	$\mathrm{mol\ m}^{-3}$
c^*	dimensionless fluid-phase concentration related to c_ref	
D_L	axial dispersion coefficient	$\mathrm{m}^2\ \mathrm{s}^{-1}$
k_S	total mass transfer coefficient based on the adsorbed phase concentration	$\mathrm{m\ s}^{-1}$
K	Langmuir isotherm parameter	$\mathrm{m}^3\ \mathrm{mol}^{-1}$
L	bed length	m
Pe	Péclet number ($= \varepsilon v L/D_\mathrm{L}$)	
q_ref	reference solid-phase concentration	$\mathrm{mol\ kg}^{-1}$
q^*	dimensionless equilibrium solid-phase concentration	
$\bar{q}^*$	dimensionless mean solid-phase concentration	
r	separation factor ($= 1/(1 + cK)$)	
s	systematic error of partition coefficient	
t	time	s
v	interstitial velocity	$\mathrm{m\ s}^{-1}$

Greek Letters

ε	void fraction of packing (extraparticle)	
Λ	partition coefficient ($= \rho_\mathrm{b} q_\mathrm{ref}/\varepsilon c_\mathrm{ref}$)	
ρ_b	bulk density of packing	$\mathrm{kg\ m}^{-3}$
τ	dimensionless time ($= vt/L$)	
ζ	dimensionless bed axial coordinate	

REFERENCES

1. Van Vliet, B. M., Weber, W. J. J., and Hozumi, H., *Water Res. 14*, 1719 (1980).
2. Hand, D. W., Crittenden, J. C., and Thacker, W. E., *J. Environ. Eng. 110*, 440 (1984).
3. Smith, E. H. and Weber, W. J. J., *Environ. Sci. Technol. 23*, 713 (1989).
4. Conder, J. R. and Young, C. L., in *Physicochemical Measurement by Gas Chromatography,* p. 353. Wiley, Chichester, 1978.
5. Tondeur, D., Kabir, H., Luo, L. A., and Granger, J., *Chem. Eng. Sci. 51*, 3781 (1996).
6. Guiochon, G., Shirazi, S. G., and Katti, A. M., *Fundamentals of Preparative and Nonlinear Chromatography.* Academic Press, Boston, 1994.
7. Weber, W. J. J. and Liu, K. T., *Chem. Eng. Commun. 6*, 49 (1980).
8. Weber, W. J. J. and Wang, C. K., *Environ. Sci. Technol. 21*, 1096 (1987).
9. Chatzopoulos, D. and Varma, A., *Chem. Eng. Sci. 50*, 127 (1995).
10. *Athena Visual Workbench. Technical Manual.* Stewart & Associates Engineering Software, Madison, Wisconsin, USA, 2001.
11. Stewart, W. E., Caracotsios, M., and Sorensen, J. P., *AIChE J. 38*, 641 (1992).
12. Caracotsios, M. and Stewart, W. E., *Comput. Chem. Eng. 19*, 1019 (1995).